18. G. S. Sandhu, W. K. Chu, M. L. Swanson, J. F. Prins, *ibid.*, p. 37.
19. D. D. Clayton, *Proc. Lunar Planet. Sci. Conf.* **12B**, 1781 (1981).
20. U. G. Jorgenson, *Nature* **332**, 702 (1988).
21. A. G. G. M. Tielens, in *Carbon in the Galaxy: Studies from Earth and Space* (National Aeronautics and Space Administration Publication CP-3061, Washington, DC, 1990), p. 59.
22. S. A. Sandford *et al.*, *Astrophys. J.* **371**, 607 (1991).
23. P. Ehrenfreund, F. Robert, L. d'Hendecourt, F. Behar, *Astron. Astrophys.* **252**, 612 (1992).
24. Y. Pendleton, S. A. Sandford, L. J. Allamandola, A. G. G. M. Tielens, K. Sellgren, in preparation.
25. W. W. Duley, A. P. Jones, D. A. Williams, *Mon. Not. R. Astron. Soc.* **236**, 709 (1989).
26. J. M. Greenberg, in *Submillimeter Wave Astronomy*, J. E. Beckman and J. P. Phillips, Eds. (Cambridge Univ. Press, Cambridge, 1982), p. 261.
27. L. J. Allamandola, S. A. Sandford, G. J. Valero, *Icarus* **76**, 225 (1988).
28. C. F. McKee, in *Interstellar Dust*, L. J. Allamandola and A. G. G. M. Tielens, Eds. (Kluwer, Dordrecht, Holland, 1989), p. 431.

29. We thank E. Anders and R. Lewis for discussion concerning the connections between the interstellar diamond band and meteoritic microdiamonds. This work was supported by National Aeronautics and Space Administration grants 199-52-12-04 and 452-33-93-03.

13 November 1992; accepted 21 January 1993

Strong, Pure, and Uniform Carbon Fibers Obtained Directly from the Vapor Phase

Frederick T. Wallenberger and Paul C. Nordine

With laser-assisted chemical vapor deposition, strong and flexible carbon fibers were obtained at high reaction chamber pressures (>1 bar) with growth rates >0.3 millimeter per second; their tensile strength (3 gigapascals) approaches that of commercial intermediate modulus carbon fibers made by conventional process routes. With the process described here, carbon fibers can be produced with superior chemical purity and structural uniformity. They may become the material of choice in currently emerging premium end uses, including carbon fiber infrared detection elements.

In 1972, Nelson and Richardson (*1*) were able to fabricate short carbon rods from methane and ethane with diameters >200 μm by laser-assisted chemical vapor deposition (LCVD) using a CO$_2$ laser and low reaction chamber pressures (<1 bar). Their process, which used laser heating of the growing fiber tip as the heat source to decompose the gaseous reactants, was slow (<10 μm s^{-1}); the carbon rods were weak and brittle because of considerable structural nonuniformities. Between 1981 and 1988, Bäuerle and others (*2*) made short carbon fibers from methane, ethylene, and acetylene by a similar LCVD process. Using an efficient Ar$^+$ laser, they obtained small fiber diameters (<25 μm), but because they also used low reaction pressures (<1 bar) they too obtained low growth rates (<20 μm s^{-1}).

In 1992, Westberg *et al.* (*3*) documented the structural complexity of small diameter carbon lines (<20 μm) that had been deposited from ethylene by a low-pressure LCVD process (<1 bar) under hot- and cold-wall conditions like those reported by Bäuerle (*2*). As shown with scanning electron microscopy (SEM) (*3*), a hot-wall material, for example, had a relatively smooth but nodular surface. Cleavage, however, showed that it had a layered and perhaps brittle core structure. Short carbon fibers were recently also obtained by metal- (versus laser-) catalyzed vapor deposition with a hot metal particle as the heat source to decompose hydrogen-hydrocarbon gases (*4*). Cylindrical hollow-core fibers result that are not visible with optical microscopy. They can be thickened and lengthened by further vapor deposition. Lengthening ceases when a metal particle is covered by pyrolytic carbon. The best summary of this technology, which yields structurally complex materials, is found in a recent review article by Tibbetts (*4*). Here, we describe the fabrication of highly uniform carbon fibers by LCVD with up to 30 times the previously documented (*1–3*) growth rates and tensile strength values that approach those of commercial intermediate modulus (IM) carbon fibers. This result was made possible through the use of an LCVD process with a reaction pressure >1 bar.

Laser-assisted chemical vapor deposition uses the focal point of a laser beam as the heat source to decompose the gaseous reactants rather than a hot reaction chamber or a hot substrate surface, as in a conventional chemical vapor deposition process. For our experiments, reaction pressures >1 bar were used. Figure 1 shows the LCVD growth of a fiber with time. Under these conditions, the hot focal point of the laser is continually adjusted in the reaction chamber (Fig. 2) to coincide with the tip of the growing fiber and to support the continuous growth of fibers directly from the vapor phase. The fabrication of microsprings and microsolenoids was recently viewed (*5*) as well as the formation of strong, small-diameter boron fibers (*6*).

The experimental apparatus (*6*) for growing the carbon fibers consisted of an optical bench with a continuous 5-W Nd–yttrium-aluminum-garnet (YAG) laser, a small reaction chamber in an enclosed laboratory hood, a system for delivering the feed gases, a microscope attached to the reaction chamber to observe and record the growth of individual fibers, and computer-operated laser power controls and stepper motors to drive the fiber pulling rate. The fiber diameters that were achieved in this process are nearly equal to the diffraction-limited laser focal spot size. The size of laser focal spot, in turn, depends on the wavelength of the laser. A small reaction chamber served as a research tool. It is suitable for producing, side-by-side, several 1.4-cm-long fiber specimens along the edge of a common substrate, a carbonized cardboard. The diameters of high-pressure–LCVD (HP-LCVD) carbon fibers made so far range from less than 10 μm to more than 30 μm.

In this apparatus, any process variable (such as pressure, feed rate, or pulling rate) can be changed within minutes, while all the others are kept constant. A simple modification of this chamber facilitates the growth of fibers up to 2 m long and the growth of potentially endless fibers directly from the vapor phase. In our experiments, carbon fibers were grown from methane and from ethylene. When grown from methane, the reactant pressures ranged from 3.4 to >7.1 bar. Individual fibers grew at a rate ranging from 9 to 331 μm s^{-1} and with diameters ranging from 20 to 170 μm. Much smaller diameter fibers may be grown at reduced laser power and increased reactor pressure. The fibers grown from ethylene

Fig. 1. Fiber growth by LCVD.

F. T. Wallenberger, Department of Materials Science and Engineering, University of Illinois, 1304 West Green Street, Urbana, IL 61801.
P. C. Nordine, Containerless Research Incorporated, 735 Carriage Way, Deerfield, IL 60015.

had diameters ranging from 10 to 40 µm. The highest growth rate for any fiber made so far from ethylene was 125 µm s^{-1}. This rate was obtained in a preliminary set of experiments at reaction chamber pressures ranging from 0.6 to 3.5 bar. Further rate increases may be possible.

The results obtained in a typical experiment with methane as the reactant and the laser power fixed at approximately 350 mW are shown in Table 1. In this experiment, no fiber growth occurred at low reactant pressures (<3.7 bar). A 1.84-fold increase in the reactant pressure from 3.7 to 6.4 bar produced an 8.1-fold increase in the fiber growth rate from 41 to 331 µm s^{-1}. Carbon fibers with still higher linear growth rates and smaller fiber diameters are expected to be possible in the high-pressure regime. The observed relation between reaction chamber pressure and fiber growth rate, but not necessarily its magnitude, is consistent with our observations concerning other carbon fiber experiments in the high-pressure regime and with observations made earlier by Bäuerle (2) regarding the low-pressure regime.

At reaction pressures between 3.7 and 4.1 bar (Table 1), the quantity *ud*, the product of the fiber growth rate (*u*) and the fiber diameter (*d*), more than tripled from 4,000 to 14,000 μm^2 s^{-1} and no carbonaceous smoke was formed. Between pressures of 4.1 and 6.4 bar, smoke formation was observed. It increased, and the value for *ud* began to approach a constant value of >21,000 μm^2 s^{-1} at pressures >6.4 bar. The magnitude of the quantity *dp*, the product of fiber diameter and reactant pressure, remained constant. A value of *ud* >21,000 μm^2 s^{-1} is apparently characteristic of the gaseous, diffusion-limited fiber growth—that is, for the fiber growth rate to be exclusively limited by the reactant diffusion through product gases at the fiber tip. More work is needed with both methane and ethylene to develop predictive process theory for carbon fiber formation in the high-pressure regime.

The HP-LCVD carbon fibers made by this process were structurally uniform and chemically pure. Figure 3, A and B, shows an SEM image for a typical fiber at a 5000-fold magnification of the surface and a cross section of a 16-µm-diameter fiber made from ethylene. Figure 3C shows the surface and cross section of a comparable pitch-based carbon fiber. The HP-LCVD fiber surface is extremely smooth, and the cross section is round. No impurity elements, fluorine through uranium, were detectable by energy dispersive x-ray spectroscopy on the surface or cross section of this fiber.

Typically, 1.4-cm-long HP-LCVD carbon fibers were subjected to tensile testing with 61-mm gauge lengths on a standard tensile tester (Instron, Canton, Massachusetts). The average tensile strength for five individual test specimens was 3.0 GPa, which thus approached that of commercial IM carbon fibers that had been manufactured from polyacrylonitrile-derived precursor fiber. In these tests, the average elongation at break for the HP-LCVD carbon fiber was high (3.0% versus 1.5% for IM fibers) and the modulus was low (180 versus 250 GPa). In related experiments, the HP-LCVD carbon fibers could be bent into very small loops before breaking. The tensile strength data obtained by Instron testing (Table 2) are believed to be representative.

Table 2. LCVD carbon fiber properties; data were obtained by Instron testing. Parentheses indicate preliminary data.

Carbon fiber type	Tensile strength (GPa)	Elongation at break (%)	Tensile modulus (GPa)
IM	3.5	1.5	250.0
HP-LCVD	3.0	(3)	(180)

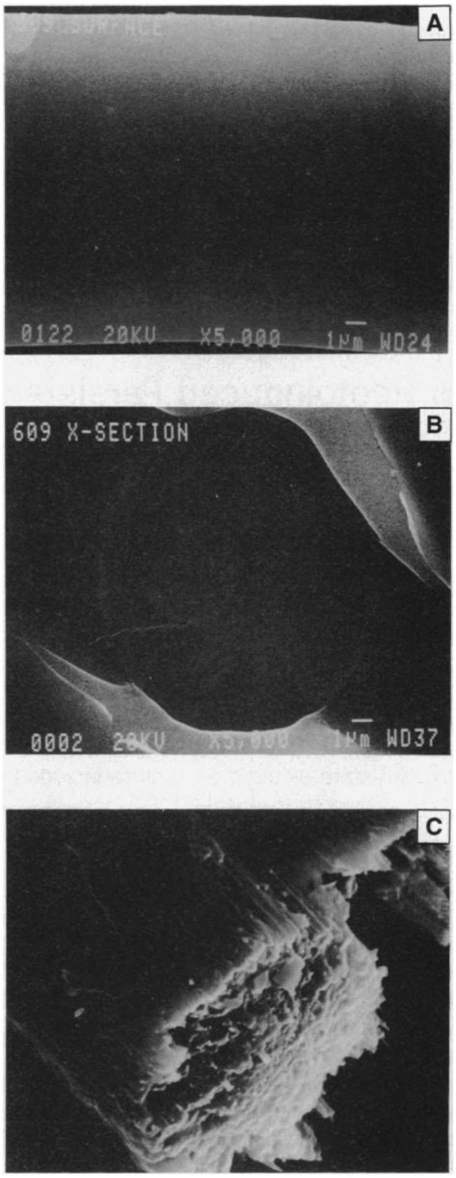

Fig. 3. SEM images of (**A**) the surface of an LCVD carbon fiber, (**B**) a cross section of a 16-µm-diameter LCVD carbon fiber, and (**C**) a cross section of a 10-µm-diameter pitch-based carbon fiber.

Fig. 2. Drawing of a typical HP-LCVD reaction chamber.

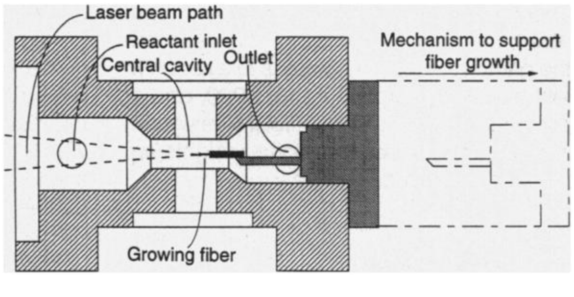

Table 1. The LCVD carbon fiber process for a typical experiment with methane as the reactant and laser power ~350 mW.

Methane pressure *p* (bar)	Growth rate *u* (µm s^{-1})	Fiber diameter *d* (µm)	Fiber growth (deposition)		
			Smoke formed?	*ud* (μm^2 s^{-1})	*dp* (µm bar)
3.4	0			0	
3.7	41	107	No	4,400	398
4.1	162	86	No	14,000	349
4.4	199	89	Yes	18,000	392
5.1	234	83	Yes	19,000	422
5.8	271	66	Yes	18,000	380
6.4	331	63	Yes	21,000	406

The modulus and elongation data are preliminary. Longer test specimens, which are not yet available, will be required to facilitate Instron testing at gauge lengths >2.5 cm and therefore to obtain representative modulus and elongation values.

In summary, strong, pure, and uniform carbon fibers were obtained by LCVD. The growth rates obtained with these fibers ($>300\ \mu m\ s^{-1}$) were comparable to those obtained with commercial melt-drawn sapphire fibers (*7*). Eventually, LCVD carbon fibers should therefore attain a price point comparable to that of melt-drawn sapphire fibers. As premium fibers, they may be suitable for currently emerging sensor markets, which have begun to use carbon fibers as functional electrical materials (*8*, *9*). For example, conventional carbon fibers were recently evaluated in Japan (*10*, *11*) and in the United States (*12*) as infrared detecting elements and intelligent infrared sensors, and the most desirable results were claimed for straight and coiled polyacrylonitrile-based carbon fibers (*12*). LCVD carbon fibers may have added value over incumbent carbon fibers because of their greater chemical purity and structural uniformity. In addition, the LCVD process can be modified to produce coiled fibers (*3*, *5*) if a coiled LCVD carbon fiber were required for a given end use.

REFERENCES

1. L. S. Nelson and N. L. Richardson, *Mater. Res. Bull.* 7, 971 (1972).
2. D. Bäuerle, *Chemical Processing with Lasers* (Springer-Verlag, Berlin, 1986), pp. 71, 93, and 224.
3. H. Westberg, M. Boman, A.-S. Norekrans, J.-O. Carlsson, *Thin Solid Films* **215**, 126 (1992).
4. G. G. Tibbetts, in *Carbon Fibers, Filaments and Composites*, J. L. Figueiredo, R. T. Baker, K. J. Hüttinger, Eds. (Kluwer, Dordrecht, Netherlands, 1990), pp. 73–94.
5. F. T. Wallenberger, lecture given at the International Workshop on Advances in Inorganic Fiber Technology, Melbourne, Australia, 13 and 14 August 1992; _____, P. C. Nordine, M. Boman, *Comp. Sci. Tech.*, in press.
6. F. T. Wallenberger and P. C. Nordine, *Mater. Lett.* **14**, 198 (1992).
7. J. T. A. Polluck, *J. Mater. Sci.* **7**, 787 (1972).
8. N. Muto *et al.*, *J. Mater. Sci. Lett.* **9**, 1269 (1990).
9. N. Muto *et al.*, *Sens. Mater.* **2**, 313 (1991).
10. H. Yanagida, in *Proc. Jpn. Ceram. Soc.* **81–90**, 81 (1991).
11. N. Muto *et al.*, *Denshi Joho Tsushin Gakkai Ronbunshi* **J74-CII**, 458 (1991).
12. C. D. E. Lakeman *et al.*, *Mater. Lett.* **13**, 330 (1992).

12 November 1992; accepted 13 January 1993

A Photoinduced Persistent Structural Transformation of the Special Pair of a Bacterial Reaction Center

N. Raja S. Reddy, Stephen V. Kolaczkowski, Gerald J. Small

Structural modification of photosynthetic reaction centers is an important approach for understanding their charge-separation processes. An unprecedented persistent structural transformation of the special pair (dimer) of bacteriochlorophyll molecules can be produced by light absorption alone. The nonphotochemical hole-burned spectra for the reaction center of *Rhodopseudomonas viridis* show that the phototransformation leads to a red shift of 150 wave numbers for the special pair's lowest energy absorption band, P960, and a comparable blue shift for a state at 850 nanometers, which can now be definitively assigned as being most closely associated with the upper dimer component. Additional insights on excited-state electronic structure include the identification of a new state.

The x-ray structures of the reaction center (RC) of the purple bacteria *Rhodopseudomonas viridis* (*1*) and *Rhodobacter sphaeroides* (*2*) have led to a burgeoning of experimental and theoretical activity directed toward an understanding of the primary charge-separation process (*3*, *4*). Although progress has been quite significant, important details are still controversial (*5*). That this is so, despite the availability of the RC structure, is a reflection of the complex and multifaceted nature of the problem; for example, a firm understanding of the electronically excited states of the RC is still lacking.

The two bacteriochlorophyll (BChl) monomers of the special pair (P) are closely juxtaposed; their pyrrole rings I overlap at an average macrocycle separation of ~3.3 Å for *Rps. viridis*. Rings I of the two monomers are essentially perfectly overlapped with the Q_y transition dipoles making an angle of 139°. It is the lowest excited $\pi\pi^*(Q_y)$ state of P, denoted as P*, that is, the primary electron donor state. This state is also designated as P_- because the structure of the special pair mandates that it is the antisymmetric linear combination of the localized excitations, $P_MP_L^*$ and $P_M^*P_L$, within the excitonic dimer model (the subscripts M and L designate protein subunits). The upper dimer component is then P_+. The RC possesses a pseudo-C_2 symmetry axis that extends from P to the nonheme Fe. The other cofactors are, in order of proximity to P, $BChl_M$ and $BChl_L$; bacteriopheophytin$_M$ ($BPheo_M$) and $BPheo_L$; and finally, the two quinones, Q_M and Q_L.

We report nonphotochemical hole burning (NPHB) for the primary donor-state absorption profile of an RC, P960 of *Rps. viridis*. The resulting 4.2-K hole spectra for the entire Q_y absorption region (Fig. 1) are distinct from the transient photochemical hole-burned (PHB) spectra (*6–8*), for which the metastable population bottleneck state used is $P^+Q_L^-$. The NPHB spectra provide fresh insights into the nature of the states that absorb in the Q_y region and reveal a remarkable photoinduced structural transformation of the special pair.

Theoretical calculations based on the phenomenological exciton model (*9*, *10*) and semiempirical quantum chemical methods (*11–13*), in which varying degrees of parameterization are used, have demonstrated that interactions between the six chromophores (quinones can be excluded) of the RC are required for an adequate description of the Q_y states. Although there is general agreement that the lowest energy excited state (P960* in *Rps. viridis*) (Fig. 2) is predominantly the lower energy excitonic component of P (P_- as defined above), the assignment of P_+ in the absorption spectrum is more problematic. Such an assignment may not even be sensible because the Q_y states higher in energy than P_- can be expected to be chromophorically mixed (*9–13*). The phenomenological exciton model does not include charge-transfer states, such as $P^+\ BChl_{M/L}^-$, and charge-resonance states ($P_M^+P_L^-$ and $P_M^-P_L^+$), which are important not only to the dynamics of charge separation (*3*, *14*) but also to the energies and physical properties, such as the permanent dipole moment (*15*) of the states absorbing in the Q_y region of the absorption spectrum.

The principles of persistent NPHB of electronic transitions in amorphous solids such as glasses and polymers have been extensively reviewed (*16*). The NPHB technique has recently been applied to the Q_y transitions of Chls of a wide variety of antenna protein complexes (*17–21*). Briefly, NPHB takes advantage of the inherent structural disorder of amorphous solids [proteins are glasslike (*22*)]. This disorder leads to significant inhomogeneous broadening ($\Gamma_I \sim 100$ to 200 cm^{-1}) of the optical absorption transition. In NPHB (*23*), selective excitation of an "isochromat" with a narrow line laser ($<<\Gamma_I$), followed by re-

---

Ames Laboratory and Department of Chemistry, Iowa State University, Ames, IA 50011.